Specification, estimation and validation of a pedestrian walking behavior model

Th. Robin * G. Antonini† M. Bierlaire * J. Cruz *

November 16, 2007

Report TRANSP-OR 071116
Transport and Mobility Laboratory
School of Architecture, Civil and Environmental Engineering
Ecole Polytechnique Fédérale de Lausanne
transp-or.epfl.ch

This report is a revised version of the report TRANSP-OR 070727 by Antonini, Bierlaire, Schneider and Robin.

*TRANSP-OR, Ecole Polytechnique Fédérale de Lausanne, CH-1015 Lausanne, Switzerland, {thomas.robin, michel.bierlaire,javier.cruz }@epfl.ch

†Business Optimization Group, Computer Science Dept., IBM Research GmbH, Zurich Research Laboratory, CH-8803 Ruschlikon, Switzerland, GAN@zurich.ibm.com

Abstract

We propose and validate a model for pedestrian walking behavior, based on discrete choice modeling. Two main types of behavior are identified: *unconstrained* and *constrained*. By unconstrained, we refer to behavior patterns which are independent from other individuals. The constrained patterns are captured by a *leader-follower* model and by a *collision avoidance* model. The spatial correlation between the alternatives is captured by a cross nested logit model. The model is estimated by maximum likelihood estimation on a real data set of pedestrian trajectories, manually tracked from video sequences. The model is successfully validated using a bi-directional flow data set, collected in controlled experimental conditions at Delft university.

1 Introduction

Pedestrian behavior modeling is an important topic in different contexts. Architects are interested in understanding how individuals move into buildings to create optimal space designs. Transport engineers face the problem of integration of transportation facilities, with particular emphasis on safety issues for pedestrians. Recent tragic events have increased the interest for automatic video surveillance systems, able to monitor pedestrian flows in public spaces, throwing alarms when abnormal behaviors occur. Special emphasis has been given to more specific evacuation scenarios, for obvious reasons. In this spirit, it is important to define mathematical models based on behavioral assumptions, tested by means of proper statistical methods. Data collection for pedestrian dynamics is particularly difficult and only few models presented in the literature have been calibrated and validated on real data sets.

Previous methods for pedestrian behavior modeling can be classified into two main categories: *microscopic* and *macroscopic* models. In the last years much more attention has focused on microscopic modeling, where each pedestrian is modeled as an agent. Examples of microscopic models are the *social forces* model in Helbing and Molnar (1995) and Helbing et al. (2002) where the authors use Newtonian mechanics with a continuous space representation to model long-range interactions, and the multi-layer utility maximization model by Hoogendoorn et al. (2002) and Daamen (2004). Blue and Adler (2001) and Schadschneider (2002) use cellular automata models, characterized by a static discretization of the space where each cell in the grid is represented by a state variable. Another microscopic approach is based on space syntax theory where people move through spaces following criteria of space visibility and accessibility (see Penn and Turner, 2002) and minimizing angular paths (see Turner, 2001). Finally, Borgers and Timmermans (1986), Whynes et al. (1996) and Dellaert et al. (1998) focus on destination and route choice problems on network topologies. For a general literature review on pedestrian behavior modeling we refer the interested reader to Bierlaire et al. (2003). For applications of pedestrian models in image analysis, we refer the reader to our previous work (Antonini et al., 2004, Venegas et al., 2005, Antonini, 2005 and Antonini, Venegas, Bierlaire and Thiran, 2006)

Leader-follower and collision avoidance behaviors play a major role in explaining pedestrian movements. Existing literature has shown the occurrence of self-organizing

processes in crowded environments. At certain levels of density, interactions between people give rise to lane formation. In order to model these effects formally, we took inspiration from previous car following models in transport engineering (including Newell, 1961, Herman and Rothery, 1965, Lee, 1966, Ahmed, 1999). The main idea in these models is that two vehicles are involved in a car following situation when a subject vehicle follows a leader, normally represented by the vehicle in front, reacting to its actions. In general, a sensitivity-stimulus framework is adopted. According to this framework a driver reacts to stimuli from the environment, where the stimulus is usually the leader relative speed. Different models differ in the specification of the sensitivity term. This modeling idea is extended here and adapted to the more complex case of pedestrian behavior. We want to stress the fact that in driver behavior modeling a distinction between acceleration and direction (or lane) is almost natural (see Toledo, 2003 and Toledo et al., 2003), being suggested by the transport facility itself, organized into lanes. The pedestrian case is more complex, the movements being two-dimensional on the walking plane, where acceleration and direction changes are not easily separable. The constrained behaviors in general, and the collision avoidance in particular are also inspired by studies in human sciences and psychology, leading to the concept of *personal space* (see Horowitz et al., 1964, Dosey and Meisels, 1969 and Sommer, 1969). Personal space is a protective mechanism founded on the ability of the individual to perceive signals from the physical and social environment. Its function is to create the spacing patterns that regulate distances between individuals and on which individual behaviors are based (Webb and Weber, 2003). Helbing and Molnar (1995) in their social forces model use the term "territorial effect". Several studies in psychology and sociology show how individual characteristics influence the perception of the space and interpersonal distance. Brady and Walker (1978) found for example that anxiety states are positively correlated with interpersonal distance. Similarly, Dosey and Meisels (1969) found that individuals establish greater distances in high-stress conditions. Hartnett et al. (1974) found that male and female individuals approached short individuals more closely than tall individuals. Other studies (Phillips, 1979 and Sanders, 1976) indicate that the other person's body size influences space.

2 Modeling framework

In this work we refer to the general framework for pedestrian behavior described by Daamen (2004). Individuals make different decisions, following a hierarchical scheme: *strategical*, *tactical* and *operational*. Destinations and activities are chosen at a strategical level; the order of the activity execution, the activity area choice and route choice are performed at the tactical level, while instantaneous decisions such as walking and stops are taken at the operational level. In this paper, we focus on pedestrian walking behavior, naturally identified by the operational level of the hierarchy just described. We consider that the strategic and tactical decisions have been exogenously made, and are interested in modeling the short range behavior in *normal* conditions, as a reaction to the surrounding environment and to the presence of other individuals. With the term "normal" we refer to non-evacuation and non-panic situations.

The motivations and the soundness of discrete choice methods have been addressed in our introductory work (Bierlaire et al., 2003, Antonini, Bierlaire and Weber, 2006, Antonini and Bierlaire, 2007). The objective of this paper is twofold. First, we aim to provide an extended disaggregate, fully estimable behavioral model, calibrated on real pedestrian trajectories manually tracked from video sequences. Second, we want to test the coherence, interpretability and generalization power of the proposed specification through a detailed validation on external data. Compared with Antonini, Bierlaire and Weber (2006), we present three important contributions: (i) we estimate the model using significantly more data representing revealed walking behavior, (ii) the model specification explicitly captures leader-follower and collision-avoidance patterns and (iii) the model is successfully validated both using cross-validation on the estimation data set, and forecasting validation on another experimental data set, not involved in the estimation process.

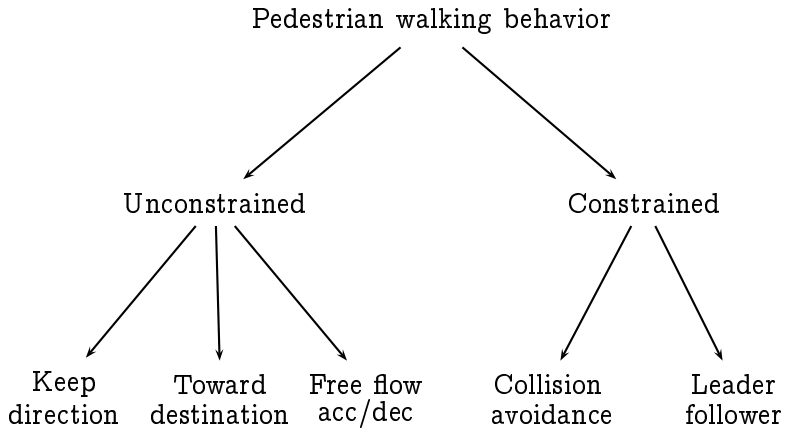

Figure 1: Conceptual framework for pedestrian walking behavior

We illustrate in Figure 1 the behavioral framework. The unconstrained decisions are independent from the presence of other pedestrians and are generated by subjective and/or unobserved factors. The first of these factors is represented by the individual's destination. It is assumed to be exogenous to the model. The second factor is represented by the tendency of people to keep their current direction, minimizing their angular displacement. Finally, unconstrained accelerations and decelerations are dictated by the individual desired speed. The implementation of these ideas is made through the three unconstrained patterns indicated in Figure 1.

We assume that behavioral constraints are induced by the interactions with the other individuals in the scene. The *collision avoidance* pattern is designed to capture the effects of possible collisions on the current trajectory of the decision maker. The *leader-follower* pattern is designed to capture the tendency of people to follow another individual in a crowd, in order to benefit from the space she is creating.

The discrete choice model introduced by Antonini, Bierlaire and Weber (2006) is extended here. The basic elements are the same and summarized below. Pedestrian

movements and interactions take place on the horizontal walking plane. The spatial resolution depends on the current speed vector of the individuals. The geometrical elements of the space model are illustrated in Figure 2.

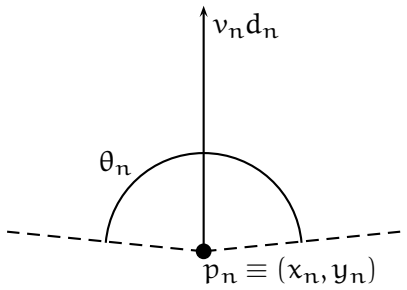

Figure 2: The basic geometrical elements of the space structure

In a given coordinate system, the current position of the decision maker n is $p_n \equiv (x_n, y_n)$, her current speed $v_n \in \mathbb{R}$, her current direction is $d_n \in \mathbb{R}^2$ (normalized such that $\|d_n\| = 1$) and her visual angle is θ_n (typically, $\theta_n = 170°$). The region of interest is situated in front of the pedestrian, ideally overlapping with her visual field. An individual-specific and adaptive discretization of the space is obtained to generate a set of possible places for the next step. Three speed regimes are considered. The individual can accelerate to 1.5 times her speed, can decelerate to half time her speed, or can maintain her current speed. Therefore, the next position will lie into one of the zones, as depicted in Figure 3(b). For a given time step t (typically, 1 second), the *deceleration* zones range from $0.25v_n t$ to $0.75v_n t$, with the center being at $0.5v_n t$, the *constant speed* zones range from $0.75v_n t$ to $1.25v_n t$, with the center being at $v_n t$, and the *acceleration* zones range from $1.25v_n t$ to $1.75v_n t$, with the center being at $1.5v_n t$. With respect to the direction, a discretization into 11 radial directions is used, as illustrated in Figure 3(a), where the angular amplitudes of the radial cones are reported in degrees.

A choice set of 33 alternatives is generated where each alternative corresponds to a combination of a speed regime v and a radial direction d, as illustrated in Figure 4. Each alternative is identified by the physical center of the corresponding cell in the spatial discretization c_{vd}, that is

$$c_{vd} = p_n + vtd, \tag{1}$$

where t is the time step. The choice set varies with direction and speed and so does the distance between an alternative's center and other pedestrians. As a consequence, differences in individual speeds are naturally mapped into differences in their relative interactions. Note that the presence of physical obstacles can be modeled by declaring the corresponding cells as not available.

3 The model

Individuals walk on a 2D plane and we model two kinds of behavior: changes in direction and changes in speed, i.e. accelerations. Five behavioral patterns are defined. In a

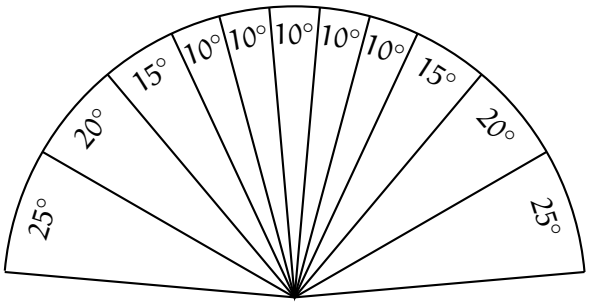

(a) Discretization of directions

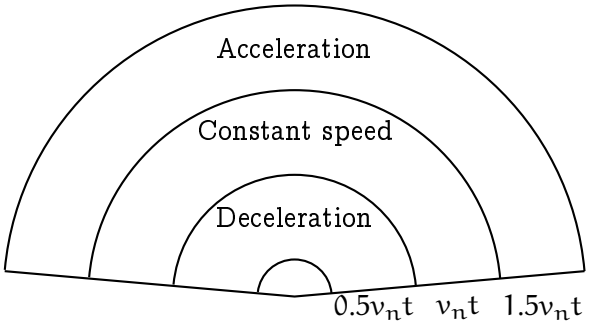

(b) Discretization of speed regimes

Figure 3: The spatial discretization.

discrete choice context, they have to be considered as terms entering the utility functions of each alternative, as reported in Equation 2. The utilities describe the space around the decision maker and under the rational behavior assumption the individual chooses that location (alternative) with the maximum utility. In the following, we discuss the different patterns and the associated assumptions in more details.

Following the framework proposed in Figure 1 we report here the systematic utility as perceived by individual n for the alternative identified by the speed regime ν and

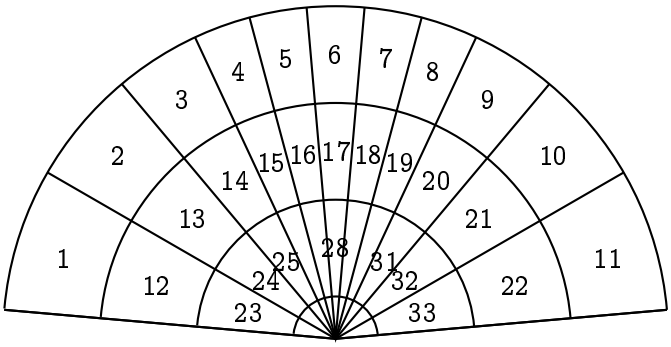

Figure 4: Choice set representation, with numbering of alternatives

direction d.

$$
\begin{aligned}
V_{\nu dn} = & \beta_{dir\_central} dir_{dn} I_{d,central} + \\
& \beta_{dir\_side} dir_{dn} I_{d,side} + \\
& \beta_{dir\_extreme} dir_{dn} I_{d,extreme} + \\
& \beta_{ddist} ddist_{\nu dn} + \\
& \beta_{ddir} ddir_{dn} + \\
& \beta_{dec} I_{v,dec} (v_n / v_{max})^{\lambda_{dec}} + \\
& \beta_{accLS} I_{n,LS} I_{v,acc} (v_n / v_{maxLS})^{\lambda_{accLS}} + \\
& \beta_{accHS} I_{n,HS} I_{v,acc} (v_n / v_{max})^{\lambda_{accHS}} + \\
& I_{v,acc} I^L_{d,acc} \alpha^L_{acc} D_L^{\rho^L_{acc}} \Delta v_L^{\gamma^L_{acc}} \Delta\theta_L^{\delta^L_{acc}} + \\
& I_{v,dec} I^L_{d,dec} \alpha^L_{dec} D_L^{\rho^L_{dec}} \Delta v_L^{\gamma^L_{dec}} \Delta\theta_L^{\delta^L_{dec}} + \\
& I_{d,d_n} I_{d,C} \alpha_C e^{\rho_C D_C} \Delta v_C^{\gamma_C} \Delta\theta_C^{\delta_C}
\end{aligned}
\qquad
\begin{aligned}
& \left.\vphantom{x}\right\} \textit{keep direction} \\
& \left.\vphantom{x}\right\} \textit{toward destination} \\
& \left.\vphantom{x}\right\} \textit{free flow acceleration} \\
& \left.\vphantom{x}\right\} \textit{leader-follower} \\
& \left.\vphantom{x}\right\} \textit{collision avoidance}
\end{aligned}
\tag{2}
$$

where all the β parameters as well as λ_{acc}, λ_{dec}, α^L_{acc}, ρ^L_{acc}, γ^L_{acc}, δ^L_{acc}, α^L_{dec}, ρ^L_{dec}, γ^L_{dec}, δ^L_{dec}, α_C, ρ_C, γ_C, δ_C are unknown and have to be estimated. Note that this specification is the result of an intensive modeling process, where many different specifications have been tested. We explain in the following the different terms of the utilities.

3.1 Keep direction

This part of the model captures the tendency of people to avoid frequent variations of the direction. People choose their next position in order to minimize the angular displacement from their current movement direction. In addition to the behavioral motivation of this factor, it also plays a smoothing role in the model, avoiding drastic changes of direction from one time period to the next. In order to capture the nonlinearity of this pattern, we include a different term for each group of directions. The "central" group, identified by the indicator $I_{d,central}$, contains the cones 5, 6 and 7 (see Figure 3), the "side" group, identified by the indicator $I_{d,side}$, contains the cones 3, 4, 8 and 9, and the

"extreme" group, identified by the indicator $I_{d,extreme}$, contains the cones 1, 2, 10 and 11.

The associated terms in the utility function are

$$\beta_{dir\_central} dir_{dn} I_{d,central} + \beta_{dir\_side} dir_{dn} I_{d,side} + \beta_{dir\_extreme} dir_{dn} I_{d,extreme} \quad (3)$$

where the variable dir_{dn} is defined as the angle in degrees between the direction d and the direction d_n, corresponding to the current direction, as shown in Figure 5. Note that the indicators guarantee that only one of these three terms is nonzero for any given alternative. We expect the β parameters to be negative.

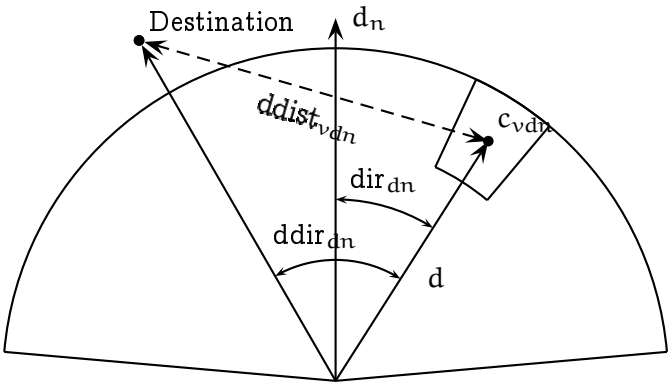

Figure 5: The elements capturing the *keep direction* and *toward destination* behaviors

3.2 Toward destination

The destination is defined as the final location that the pedestrian wants to reach. To be coherent with the general framework introduced in Section 1, we assume that the destination choice is performed at the strategical (or possibly tactical) level in the hierarchical decision process, and is therefore exogenous in this model. Such a higher level choice is naturally reflected on the short term behavior as the tendency of individuals to choose, for the next step, a spatial location that minimize both the angular displacement and the distance to the destination.

This behavior is captured by the term

$$\beta_{ddist} ddist_{vdn} + \beta_{ddir} ddir_{dn} \quad (4)$$

where the variable $ddist_{vdn}$ is defined as the distance (in meters) between the destination and the center of the alternative C_{vdn}, while $ddir_{dn}$ is defined as the angle in degrees between the destination and the alternative's direction d, as shown in Figure 5. We expect a negative sign for both the β_{ddir} and β_{ddist} parameters.

3.3 Free flow acceleration

In free flow conditions the behavior of the individual is driven by her desired speed. The acceleration is then a function of the difference between current speed and desired

speed. However, this variable is unobserved and it cannot be introduced explicitly in the model. As a consequence, we assume that the utility for acceleration is dependent on the current speed. Increasing speed corresponds to decreasing utility for further accelerations. In order to reflect that a parameter varies with speed v_n, we use the specification

$$\beta = \bar{\beta} \left(\frac{v_n}{v_{ref}} \right)^{\lambda}. \tag{5}$$

Note that

$$\lambda = \frac{\partial \beta}{\partial v_n} \frac{v_n}{\beta}$$

can be interpreted as the elasticity of the parameter β with respect to the speed v_n. The value of v_{ref} is arbitrary, and determines the reference speed corresponding to $\bar{\beta}$.

In our context, we define such a term for the parameters associated with deceleration

$$\beta_{dec} I_{v,dec} (v_n / v_{max})^{\lambda_{dec}} \tag{6}$$

where $I_{v,dec}$ is one if v corresponds to a deceleration, and zero otherwise, and the reference speed is selected to be the maximum speed observed $v_{max} = 4.84$ (m/s). The impact of this term on the utility is illustrated on Figure 6(a) (the estimated values of the parameters have been used to generate Figure 6). It shows that the utilities of the alternatives associated with deceleration are very low when the pedestrian already walks slowly. For higher speeds, this term has basically no impact on the utility.

For the acceleration, we have introduced two such terms, one for lower speeds (less or equal to 5km/h = 1.39 m/s), and one for higher speeds.

$$\beta_{accLS} I_{n,LS} I_{v,acc} (v_n / v_{maxLS})^{\lambda_{accLS}} + \beta_{accHS} I_{n,HS} I_{v,acc} (v_n / v_{max})^{\lambda_{accHS}} \tag{7}$$

where $I_{n,LS}$ is one if the individual's current speed is less or equal to 1.39 and zero otherwise, $I_{n,HS} = 1 - I_{n,LS}$, and the reference speed for low speeds $v_{maxLS} = 1.39$. The indicator $I_{v,acc}$ is 1 if the alternative corresponds to an acceleration and 0 otherwise. We expect negative signs for β_{accHS}, β_{accLS}, β_{dec} and λ_{dec} parameters, while a positive sign is expected for λ_{accLS} and λ_{accHS}. The impact of this term on the utility is illustrated on Figure 6(b), where the two parts of the curve (low and high speed) are represented. It appears clearly that the role of the second part is to avoid a too dramatic penalization of acceleration for high speeds.

3.4 Leader-follower

We assume that the decision maker is influenced by leaders. In our spatial representation 11 radial cones partition the space (see Figure 3). In each of these directions a possible leader can be identified among a set of *potential leaders*. A potential leader is an individual which is inside a certain region of interest, *not so far* from the decision maker and with a moving direction *close enough* to the direction of the radial cone where she is. Among the set of potential leaders for each radial direction, one of them is selected as leader for that direction (the closest to the decision maker). Once identified, the leader induces an attractive interaction on the decision maker. Similarly to car

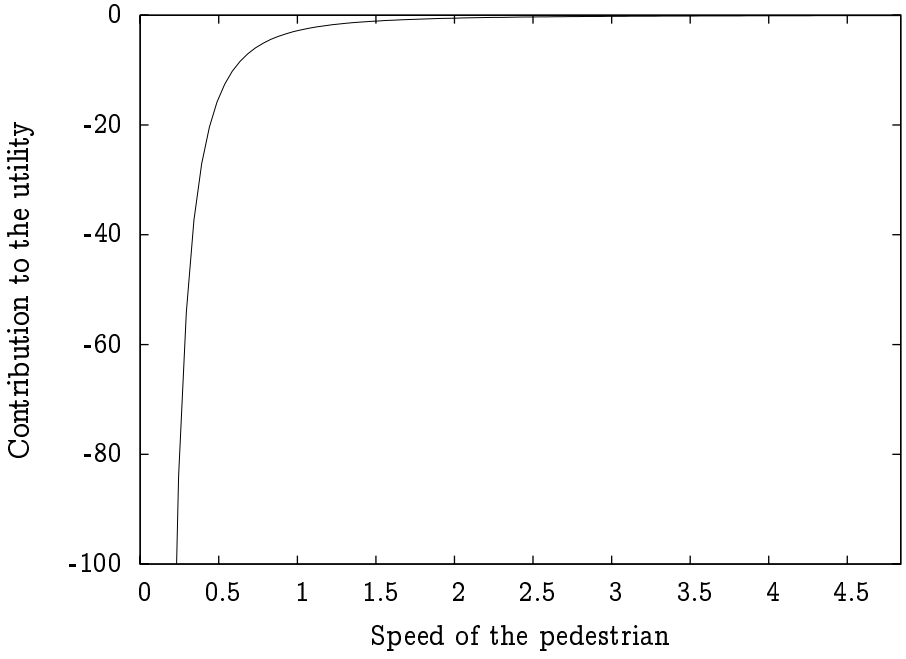

(a) Deceleration

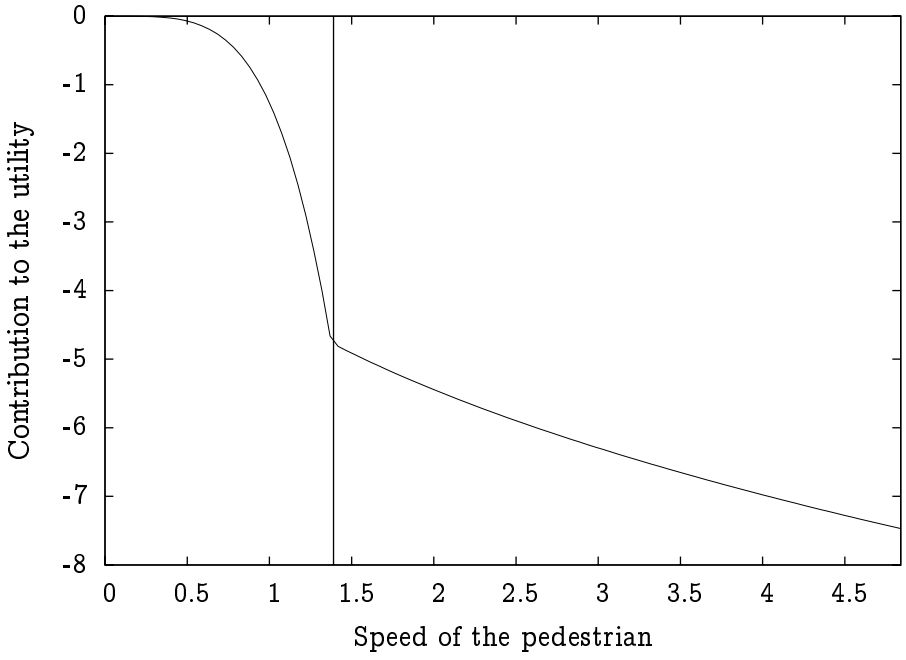

(b) Acceleration

Figure 6: Impact of the free flow acceleration terms on the utility

following models, a leader acceleration corresponds to a decision maker acceleration. The leader-follower model is given by the following terms

$$I_{v,acc} I^L_{d,acc} \alpha^L_{acc} D_L^{\rho^L_{acc}} \Delta v_L^{\gamma^L_{acc}} \Delta\theta_L^{\delta^L_{acc}} + I_{v,dec} I^L_{d,dec} \alpha^L_{dec} D_L^{\rho^L_{dec}} \Delta v_L^{\gamma^L_{dec}} \Delta\theta_L^{\delta^L_{dec}}. \quad (8)$$

It is described by a *sensitivity/stimulus* framework. The leader for each direction is chosen considering several *potential leaders* (represented by light gray circles in Figure 7). An individual k is defined as a potential leader based on the following indicator function:

$$I^k_g = \begin{cases} 1, & \text{if } d_l \le d_k \le d_r \text{ (is in the cone),} \\ & \text{and } 0 < D_k \le D_{th} \text{ (not too far),} \\ & \text{and } 0 < |\Delta\theta_k| \le \Delta\theta_{th} \text{ (walking in almost the same direction),} \\ 0, & \text{otherwise,} \end{cases}$$

where d_l and d_r represent the bounding left and right directions of the cone in the choice set (defining the region of interest) while d_k is the direction identifying the position of pedestrian k . D_k is the distance between pedestrian k and the decision maker, $\Delta\theta_k = \theta_k - \theta_d$ is the difference between the movement direction of pedestrian k (θ_k) and the angle characterizing direction d, i.e. the direction identifying the radial cone where individual k lies (θ_d). The two thresholds D_{th} and $\Delta\theta_{th}$ are fixed at the values $D_{th} = 5D_{max}$, where D_{max} is the radius of the choice set, and $\Delta\theta_{th} = 10$ degrees. We assume an implicit *leader choice* process, executed by the decision maker herself and modeled choosing as leader for each direction the potential leader at the minimum distance $D_L = \min_{k\in K}(D_k)$, illustrated in Figure 7 by the darker circle. Once the leader is identified, we compare her speed. The indicator $I^L_{d,acc}$ is one if the leader in the code d has been identified with a speed larger than v_n, and zero otherwise. Similarly, $I^L_{d,dec} = 1 - I^L_{d,acc}$ is one if the leader in cone d has been identified with a speed lower than v_n, and zero otherwise. Finally, the indicator functions $I_{v,acc}$ and $I_{v,dec}$ discriminate between accelerated and decelerated alternatives, as for the free flow acceleration model. The underlying assumption is that faster leaders will have an impact on the accelaration, while slower leaders will have an impact on the deceleration.

For a given leader, the sensitivity is described by

$$\text{sensitivity} = \alpha^L_g D_L^{\rho^L_g} \quad (9)$$

where D_L represents the distance between the decision maker and the leader. The parameters α^L_g and ρ^L_g have to be estimated and $g = \{acc, dec\}$ indicates when the leader is accelerating with respect to the decision maker. Both α^L_{acc} and α^L_{dec} are expected to be positive while a negative sign is expected for ρ^L_{acc} and ρ^L_{dec}.

The decision maker reacts to stimuli coming from the chosen leader. We model the stimulus as a function of the leader's relative speed Δv_L and the leader's relative direction $\Delta\theta_L$ as follows:

$$\text{stimulus} = \Delta v_L^{\gamma^L_g} \Delta\theta_L^{\delta^L_g} \quad (10)$$

with $\Delta v_L = |v_L - v_n|$, where v_L and v_n are the leader's speed module and the decision maker's speed module, respectively. The variable $\Delta\theta_L = \theta_L - \theta_d$, where θ_L represents

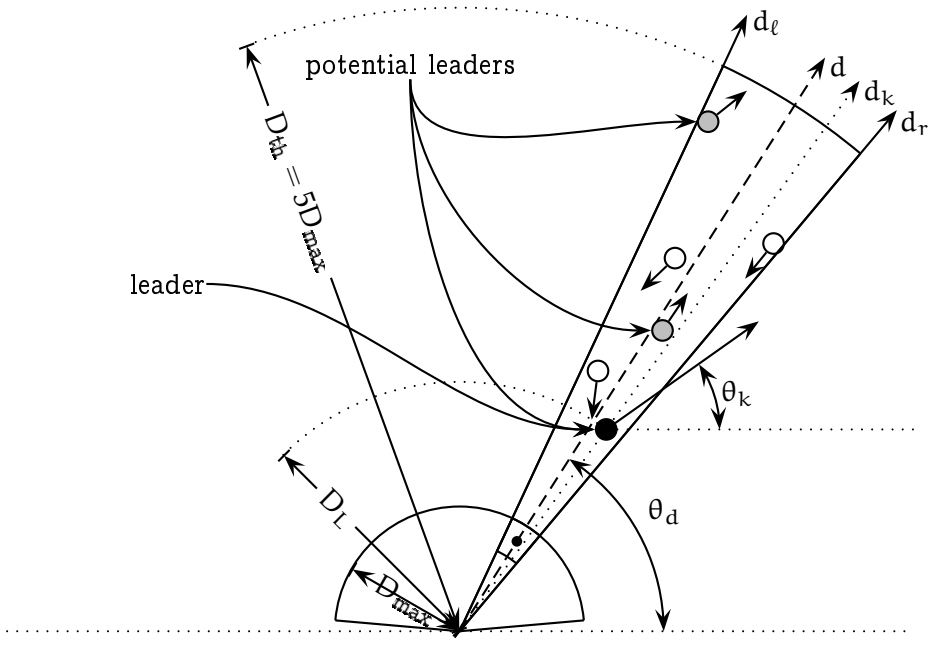

Figure 7: Leader and potential leaders in a given cone

the leader's movement direction and θ_d is the angle characterizing direction d, as shown in Figure 7. Positive signs are expected for both the γ^L_{acc} and γ^L_{dec} parameters, while we expect a negative sign for both the δ^L_{acc} and δ^L_{dec}. A leader acceleration induces a decision maker's acceleration. A substantially different movement direction in the leader reduces the influence of the latter on the decision maker. Note that in the final specification, the parameter δ^L_{dec} appeared not to be significantly different from 0. Therefore, we have decided to remove it from the model for the final estimation. The specification (8) becomes

$$I_{v,acc} I^L_{d,acc} \alpha^L_{acc} D_L^{\rho^L_{acc}} \Delta v_L^{\gamma^L_{acc}} \Delta\theta_L^{\delta^L_{acc}} + I_{v,dec} I^L_{d,dec} \alpha^L_{dec} D_L^{\rho^L_{dec}} \Delta v_L^{\gamma^L_{dec}}. \quad (11)$$

3.5 Collision avoidance

This pattern captures the effects of possible collisions on the decision maker trajectory. For each direction in the choice set, a collider is identified among a set of *potential colliders*. Another individual is selected as a potential collider if she is inside a certain region of interest, *not so far* from the decision maker and walking in the opposite direction. The collider for a radial direction is chosen from the set of potential colliders for that direction as the individual whose walking direction forms the larger angle with the decision maker walking direction. This pattern is associated with repulsive interactions in the obvious sense that pedestrians change their current direction to avoid collisions with other individuals. The collision avoidance model is given by the following term

$$I_{d,d_n} I_{d,C} \alpha_C e^{\rho_C D_C} \Delta v_C^{\gamma_C} \Delta\theta_C^{\delta_C}. \quad (12)$$

The collider for each direction is chosen considering several *potential colliders*, as shown in Figure 8. An individual k is defined as a potential collider based on the following indicator function:

$$I_C^k = \begin{cases} 1, & \text{if } d_l \le d_k \le d_r \text{ (is in the cone),} \\ & \text{and } 0 < D_k \le D'_{th} \text{ (not too far),} \\ & \text{and } \frac{\pi}{2} \le |\Delta\theta_k| \le \pi \text{ (walking in the other direction),} \\ 0, & \text{otherwise,} \end{cases}$$

where d_l, d_r and d_k are the same as those defined for the leader-follower model. D'_k is the distance between individual k and the center of the alternative, $\Delta\theta_k = \theta_k - \theta_{d_n}$ is the difference between the movement direction of pedestrian k, θ_k, and the movement direction of the decision maker, θ_{d_n}. The value of the distance threshold is now fixed to $D'_{th} = 10D_{max}$. We use a larger value compared to the leader-follower model, assuming the collision avoidance behavior being a longer range interaction, happening also at a lower density level. We assume an implicit *collider choice* process, which is deterministic and decision-maker specific. Among the set of K_d potential colliders for direction d, a collider is chosen in each cone as that individual having $\Delta\theta_C = \max_{k \in K_d} |\Delta\theta_k|$. The indicator $I_{d,C} = 1$ if a collider has been identified, and 0 otherwise. Finally, the collision avoidance term is included in the utility functions of all the alternatives. So, the indicator function I_{d,d_n} is equal to 1 for those alternatives that are not in the current direction ($d \neq d_n$), 0 otherwise.

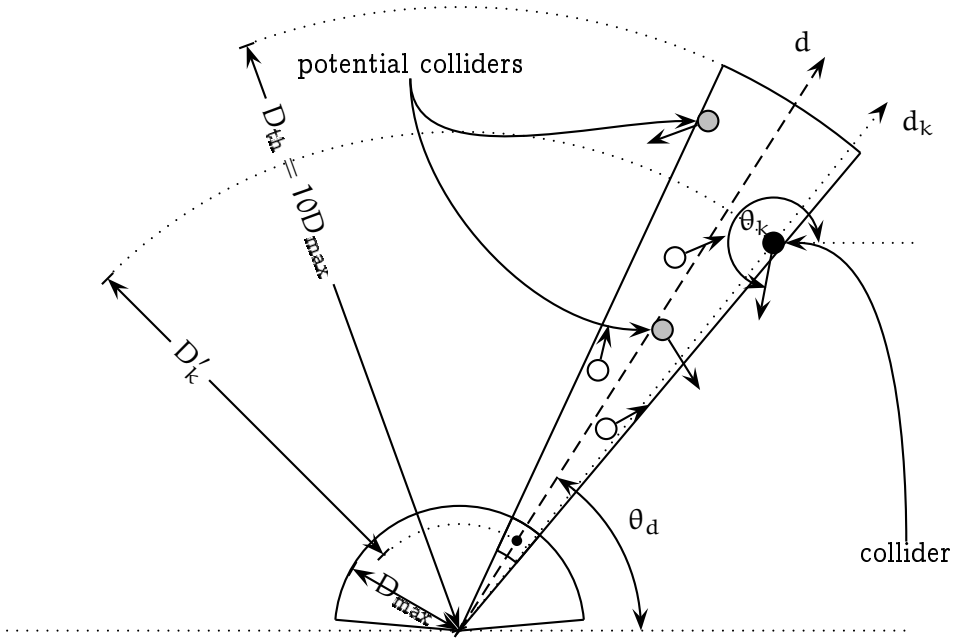

Figure 8: Collider and potential colliders in a given cone

We apply a similar sensitivity/stimulus framework, where the sensitivity function is

defined as

$$\text{sensitivity} = \alpha_C e^{\rho_C D_C} \tag{13}$$

where the parameters α_C and ρ_C, that have to be estimated, are expected to have both a negative sign and D_C is the distance between the collider position and the center of the alternative. The decision maker reacts to stimuli coming from the collider. We model the stimulus as a function of two variables:

$$\text{stimulus} = \Delta v_C^{\gamma_C} \Delta\theta_C^{\delta_C} \tag{14}$$

with $\Delta\theta_C = \theta_C - \theta_{d_n}$, where θ_C is the collider movement direction and θ_{d_n} is the decision maker movement direction, and $\Delta v_C = v_C + v_n$, where v_C is the collider's speed module and v_n is the decision maker's speed module. The parameters γ_C and δ_C have to be estimated and a positive sign is expected for both of them. Individuals walking against the decision maker at higher speeds and in more frontal directions (higher $\Delta\theta_C$) generate stronger reactions, weighted by the sensitivity function.

Note that in the final specification, the parameters γ_C and δ_C appeared not to be significantly different from 0. Therefore, we have decided to remove them from the model for the final estimation. The specification involves only the sensitivity part (13).

3.6 The error term

We use a cross nested logit (CNL) model (see, among others, Wen and Koppelman, 2001, Bierlaire, 2006, Abbe et al., 2007) specification. Such a model allows flexible correlation structures in the choice set, keeping a closed form solution. The CNL being a Multivariate Extreme Value model (MEV, see McFadden, 1978), the probability of choosing alternative i within the choice set C is:

$$P(i|C) = \frac{y_i \frac{\partial G}{\partial y_i}(y_1, ..., y_J)}{\mu G(y_1, ..., y_J)} \tag{15}$$

where J is the number of alternatives in C, $y_j = e^{V_j}$ with V_j the systematic part of the utility described by (2) and G is the following generating function:

$$G(y_1, ..., y_J) = \sum_{m=1}^{M} \left(\sum_{j \in C} (\alpha_{jm}^{1/\mu} y_j)^{\mu_m} \right)^{\frac{\mu}{\mu_m}} \tag{16}$$

where M is the number of nests, $\alpha_{jm} \geq 0, \forall j, m$, $\sum_{m=1}^{M} \alpha_{jm} > 0, \forall j$, $\mu > 0$, $\mu_m > 0, \forall m$ and $\mu \leq \mu_m, \forall m$. This formulation leads to the following expression for the choice probability formula, using $y_i = e^{V_i}$:

$$P(i|C) = \sum_{m=1}^{M} \frac{\left(\sum_{j \in C} \alpha_{jm}^{\mu_m/\mu} y_j^{\mu_m} \right)^{\frac{\mu}{\mu_m}}}{\sum_{n=1}^{M} \left(\sum_{j \in C} \alpha_{jn}^{\mu_n/\mu} y_j^{\mu_n} \right)^{\frac{\mu}{\mu_n}}} \frac{\alpha_{im}^{\mu_m/\mu} y_i^{\mu_m}}{\sum_{j \in C} \alpha_{jm}^{\mu_m/\mu} y_j^{\mu_m}} \tag{17}$$

We assume a correlation structure depending on the speed and direction and we identify five nests: *accelerated*, *constant speed*, *decelerated*, *central* and *not central*.

(a) Japanese scenario

Figure 9: A frame from the Japanese video

We fix the degrees of membership to the different nests (α_{jm}) to the constant value 0.5. The parameter μ is normalized to 1, and the nest parameters μ_m are estimated. Note that the parameters associated with the deceleration nest has been constrained to 1 in the final specification, as it did not appear to be significantly different to that value.

We conclude this section by emphasizing that the above specification ignores heterogeneity in the population. Characteristics such as age, sex, weight, height (among others) probably influence the spatial perception, interpersonal distance and human-human interactions. However, given the nature of the data (trajectories) it is not possible to take them into account in the model. Therefore, a specification with unobserved heterogeneity captured by random coefficient in a panel data setup would have been appropriate. However, the complexity of this specification did not allow us to estimate the model with a sufficiently high number of draws.

4 Data

The data set used to estimate the model consists of pedestrian trajectories manually tracked from video sequences.

It has been collected in Sendai, Japan, on August 2000 (see Teknomo et al., 2000, Teknomo, 2002). The video sequence has been recorded from the 6th floor of the JTB parking building (around 19 meters height), situated at a large pedestrian crossing point. Two main pedestrian flows cross the street, giving rise to a large number of interactions. A frame extracted from this video is represented in Figure 9.

In this context, 190 pedestrian trajectories have been manually tracked at a rate of 2 processed frames per second, for a total number of 10200 position observations. The mapping between the image plane and the walking plane was performed by Arsenal Research (Bauer, 2007) using a 3D-calibration with the standard DLT algorithm (Shapiro, 1978). The reference system on the walking plane has the origin arbitrarily

placed on the bottom left corner of the zebra crossing. The x axis represents the width of the crossing while the y axis is the crossing length.

For each frame, the following information for each visible pedestrian has been collected: (i) the time t corresponding to the frame f (in this case $t = f/2$), (ii) the pedestrian identifier n, and (iii) the coordinates $p_n^f = (x_n^f, y_n^f)$ identifying the location of the pedestrian in the walking plane.

From these raw data, we have first derived the current direction and speed of each pedestrian using the current and the previous frames, that is

$$\begin{aligned} d_n &= p_n^f - p_n^{f-1}, \\ v_n &= \|d_n\|/0.5 = 2\|d_n\|. \end{aligned}$$

In Figure 10 we report the speed histogram and in Table 1 the speed statistics.

Then, a specific choice set (see Figure 4) has been constructed for each pedestrian, based on (1) where $t = 1$ sec (that is, 2 frames), $v = v_n$ for constant speed alternatives, $v = 0.5v_n$ for decelerated alternatives, $v = 1.5v_n$ for accelerated alternatives, $d = d_n$ for alternatives in cone 6 (alt. 6, 17, 28), and $d = \mathrm{rot}(d_n, \zeta)$ is obtained by rotating d_n around p_n with an angle ζ corresponding to the cone, that is

Cone 1:	$\zeta = 72.5°$,	Cone 11:	$\zeta = -72.5°$,
Cone 2:	$\zeta = 50°$,	Cone 10:	$\zeta = -50°$,
Cone 3:	$\zeta = 32.5°$,	Cone 9:	$\zeta = -32.5°$,
Cone 4:	$\zeta = 20°$,	Cone 8:	$\zeta = -20°$,
Cone 5:	$\zeta = 10°$,	Cone 7:	$\zeta = -10°$.

For each cell in the choice set, each variable in (2) has then been computed based on the descriptions in Section 3. Note that the destination of each individual is defined by her location in the last frame where she is visible. Finally, the chosen alternative has been identified as the cell containing the pedestrian's location after 1 second, that is p_n^{f+2}. In the rare instances where p_n^{f+2} did not belong to any cell (because of numerical errors due to poor image resolution, or extreme speed variations), the corresponding piece of data was removed from the sample (for a total of 919 observations). We represent in Figure 11 selected generated choice sets on a given trajectory (representing them all would have been unreadable on the figure).

We obtain a total of 9281 observations for 190 pedestrians . In Figure 12 we report the frequency of the revealed choices as observed in the data set. The three peaks in the distributions arise on the central alternatives (6, 17, 28), as expected. Note that cells 1, 12, 23 and 33 are never chosen in this sample. The repartition of the observations across the nests is detailed in Table 2.

5 Estimation results

We report in Table 3 the estimation results. The parameters have been estimated using the Biogeme package (Bierlaire, 2003, biogeme.epfl.ch).

All estimates have the expected sign. Note that the parameter associated with the deceleration nest was clearly insignificant, and fixed to 1. The p-value for the central

Mean	1.31
Standard Error	0.012
Median	1.27
Mode	1.28
Standard Deviation	0.37
Minimum	0.43
Maximum	4.84

Note: *standard error* is the estimated standard deviation of the sample mean

Table 1: Speed statistics(m/sec)

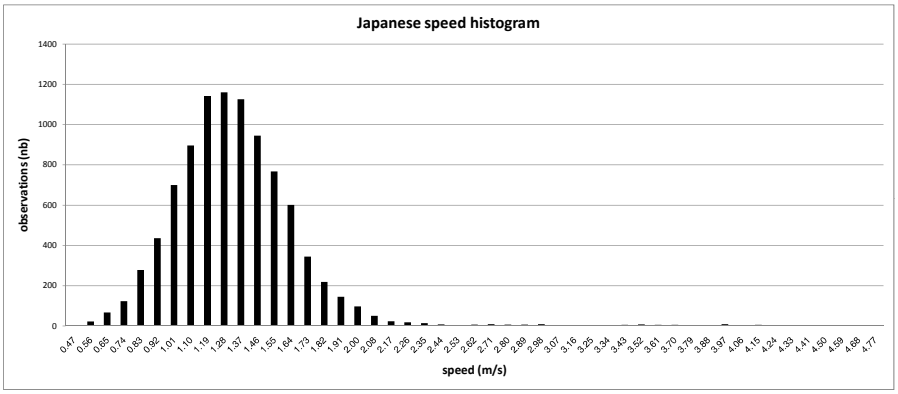

Figure 10: Speed histogram

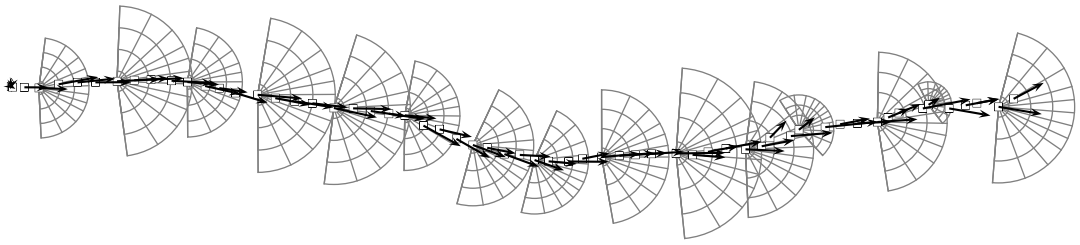

Figure 11: Example of one manually tracked trajectory with choice sets

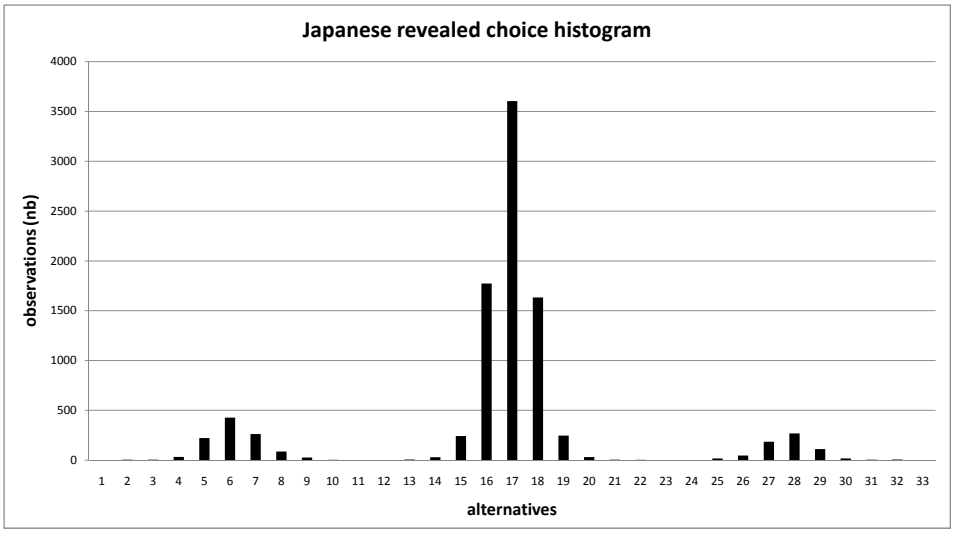

Figure 12: Revealed choices histograms

Nest	# steps	% of total
acceleration	1065	11.48%
constant speed	7565	81.51%
deceleration	651	7.01%
central	4297	46.30%
not central	4984	53.70%

Table 2: Number of chosen steps in each nest for the real data set

nest parameter is 0.27 (t-test = 1.11) which cannot be used for a clear rejection of the null hypothesis that the true value is 1.0. However, to avoid a potential misspecification, we prefer not constraining it to 1 in the final model.

In addition to the proposed model, we analyze also a simple model, where the utility of each alternative is represented only by an alternative specific constant. This constant-only model perfectly reproduces the observed shares in the sample, with 28 parameters. Indeed, there are 33 alternatives, minus 4 which are never chosen, minus one constant normalized to 0. With this model, the loglikelihood drops from -13997.27 down to -17972.03, illustrating the statistical significance of the proposed specification. Note that a classical likelihood ratio test is not appropriate here, as the hypotheses are not nested. We believe that a more rigorous test is not really necessary given the huge jump in loglikelihood value.

6 Model validation

Two data sets are used for validation: the Japanese data set used for estimation and described in Section 4, and a data set collected in the Netherlands, which has not been involved at all in the estimation of the parameters.

Variable name	Coefficient estimate	t test 0	Variable name	Coefficient estimate	t test 0	t test 1
β_{ddir}	-0.0790	-24.53	ρ^{L}_{acc}	-0.489	-2.19	
β_{ddist}	-1.55	-11.66	γ^{L}_{acc}	0.625	2.87	
$\beta_{\text{dir\_extreme}}$	-0.0326	-9.30	α^{L}_{dec}	3.69	6.90	
$\beta_{\text{dir\_side}}$	-0.0521	-21.87	ρ^{L}_{dec}	-0.663	-7.11	
$\beta_{\text{dir\_central}}$	-0.0252	-8.74	γ^{L}_{dec}	0.652	6.19	
β_{accLS}	-4.97	-22.61	δ^{L}_{acc}	-0.171	-2.33	
β_{accHS}	-7.47	-5.21	α_{C}	-0.00639	-9.82	
β_{dec}	-0.0630	-2.40	ρ_{C}	-0.239	-8.28	
λ_{accLS}	4.16	15.94	μ_{acc}	1.66	9.73	3.88
λ_{accHS}	0.358	2.09	μ_{const}	1.50	13.46	4.48
λ_{dec}	-2.41	-8.43	μ_{central}	2.35	1.93	1.11
α^{L}_{acc}	0.942	2.28	$\mu_{\text{not\_central}}$	1.75	9.46	4.04
Sample size = 9281			Init log-likelihood = -32451			
Nbr of estimated parameters = 24			Final log-likelihood = -13997.27			
$\bar{\rho}^2 = 0.568$			Likelihood ratio test = 36907			

Table 3: **CNL** estimation results for the Japanese data set

In Section 6.1, we apply the model on the Japanese data set, and compare the predicted choices with the observed ones. In Section 6.2, we test the robustness of the model specification by performing cross-validation, where a subset of the Japanese data set is saved for validation, and the model is estimated on the rest. Finally, in Section 6.3, we apply both our model, and a simple constant-only model on the data set collected in the Netherlands.

6.1 Japanese data set: validation of the model

We first apply our model with the parameters described in Table 3 on the Japanese data set, using the Biosim package (Bierlaire, 2003). For each observation n, we obtain a probability distribution $P_n(i)$ over the choice set.

Figure 13 represents the histogram of the probability value $P_n(i^*_n)$ assigned by the model to the chosen alternative i^*_n of each observation n, along with the hazard value $1/33$ (where 33 is the number of alternatives). We consider observations below this threshold as outliers. There are only 7.13% of them. As a comparison, there are 19.90% of outliers with the constant-only model.

The top part of Figure 14 reports, for each i, $\sum_n P_n(i)$, and the bottom part reports $\sum_n y_{in}$, where y_{in} is 1 if alternative i is selected for observation n, 0 otherwise. As expected, the two histograms are similar, indicating no major specification error.

This is confirmed when alternatives are aggregated together, by directions (see Table 4) and by speed regimes (see Table 5). For a group Γ of alternatives, the quantities

$$\begin{aligned} M_\Gamma &= \sum_n \sum_{i\in\Gamma} P_n(i), \\ R_\Gamma &= \sum_n \sum_{i\in\Gamma} y_{in}, \end{aligned}$$

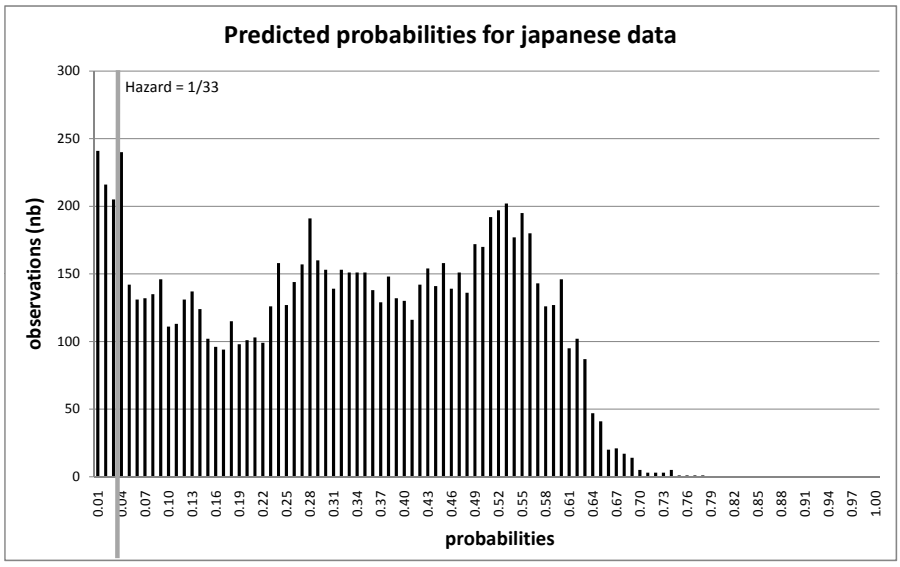

Figure 13: Predicted probabilities of the Japanese data

and

$$(M_\Gamma - R_\Gamma)/R_\Gamma$$

are reported in columns 3, 4 and 5, respectively, of these tables.

The relative errors showed in Table 4 and Table 5 are low, except for groups of alternatives with few observations, that is groups corresponding to extreme left and extreme right directions.

Cone	Γ	M_Γ	R_Γ	$(M_\Gamma - R_\Gamma)/R_\Gamma$
Front	$5-7, 16-18, 27-29$	8489.27	8481	0.0010
Left	$3, 4, 14, 15, 25, 26$	349.67	367	-0.0472
Right	$8, 9, 19, 20, 30, 31$	415.45.	407	0.0208
Extreme left	$1, 2, 12, 13, 23, 24$	12.29	10	0.2296
Extreme right	$10, 11, 21, 22, 32, 33$	14.30	16	-0.1059

Table 4: Predicted (M_Γ) and observed (R_Γ) shares for alternatives grouped by directions with the Japanese data set.

6.2 Japanese data set: validation of the specification

In order to test the proposed specification, we have performed a cross validation done on the Japanese data set. It consists in splitting the data set into 5 subsets, each containing 20% of the observations. We perform 5 experiments. For each of them, one of the five subsets is saved for validation purposes, and the model is re-estimated on the remaining 4 subsets. The same procedure has been applied with the constant-only model. The proportion of outliers for each experiment is reported in table 6. We observe that they are consistent with 7.13% (for our model) and 19.90% (for the constant-only

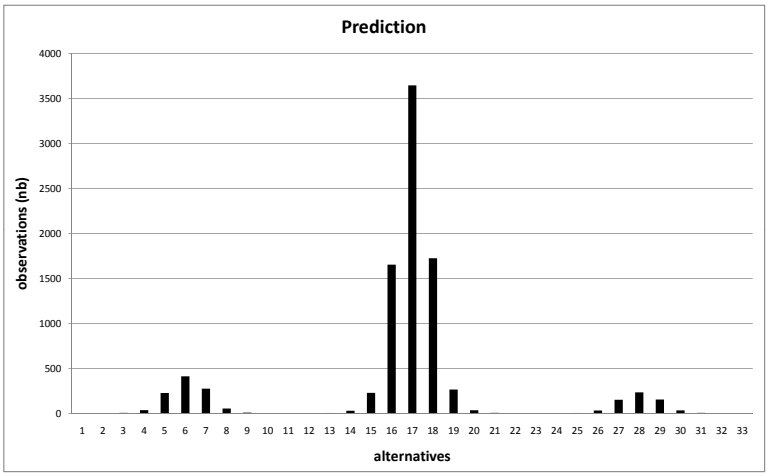

(a) Predicted shares

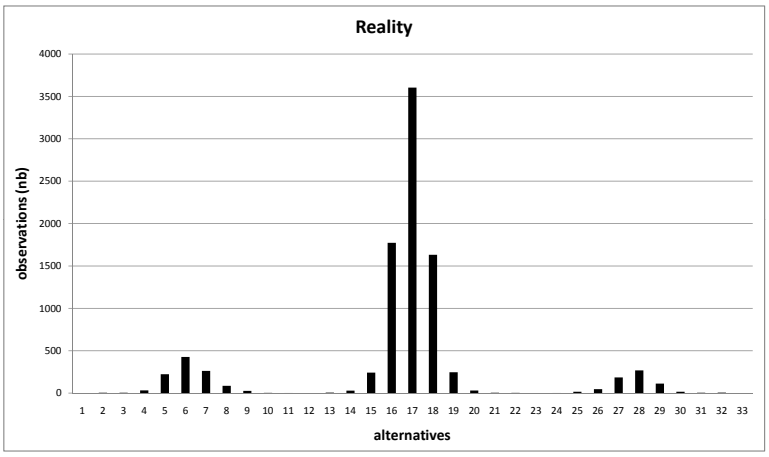

(b) Observed shares

Figure 14: Predicted and observed shares for the Japanese data set

Area	Γ	M_Γ	R_Γ	$(M_\Gamma - R_\Gamma)/R_\Gamma$
acceleration	$1-11$	1041.50	1065	-0.0221%
constant speed	$12-22$	7606.49	7565	0.0055
deceleration	$23-33$	633.02	651	-0.0276%

Table 5: Predicted and observed shares for alternatives grouped by speed regime with the Japanese data set.

model) of outliers obtained with the complete data set, illustrating the robustness of the specification.

Model	Exp. 1	Exp. 2	Exp. 3	Exp. 4	Exp. 5
Proposed spec.	8.78%	6.36%	7.60%	7.87%	5.87%
Constant only	20.79%	20.70%	17.13%	19.88%	18.64%

Table 6: Summary of the cross-validation performed on the Japanese data set

The above analysis indicates a good specification and performance of the model. However, it is not sufficient to fully validate it. Consequently, we perform now the same analysis on a validation data set, not involved in the estimation of the model.

6.3 Dutch data set: validation of the model

This data set has been collected at Delft University, in the period 2000-2001 (Daamen and Hoogendoorn, 2003, Daamen, 2004) where volunteer pedestrians were called to perform specific walking tasks in a controlled experimental setup.

For the purpose of our validation procedure we use the subset of the Dutch data set corresponding to a bi-directional flow. This situation is the experimental version of the Japanese data set, which corresponds to a walkway. The subset includes 724 subjects for 47481 observed positions, collected by means of pedestrian tracking techniques on video sequences, at a frequency of 10Hz, that is 10 frames per second. In Figure 15 we report one frame from the experimental scenario.

For each frame, we have collected for each visible pedestrian the time t corresponding to the frame f (in this case $t = f/10$), the pedestrian identifier n, and the coordinates $p_n^f = (x_n^f, y_n^f)$ identifying the location of the pedestrian in the walking plane. From these raw data, we have derived the current direction and speed of each pedestrian using the current and the previous frames, that is

$$\begin{aligned} d_n &= p_n^f - p_n^{f-1}, \\ v_n &= \|d_n\|/0.1 = 10\|d_n\|. \end{aligned}$$

Consistently with the model assumptions, the chosen alternative has been identified as the cell containing the pedestrian's location after 1 second, that is p_n^{f+10}.

The repartition of the observations across nests is detailed in Table 7. We note the very low number of decelerations and accelerations, probably due to the experimental nature of the data.

We compare the observed choices for the Japanese and the Dutch data set in Table 8 and Figure 16. Table 8 reports the percentage of observations for cells at the extreme left of the choice set (alts. 1, 2, 12, 13, 23, 24), the left part (alts. 3, 4, 14, 15, 25, 26), the front (alts. 5-7, 16-18, 27-29), the right (alts. 8, 9, 19, 20, 30, 31) and the extreme right (10, 11, 21, 22, 32, 33). Figure 16 reports normalized observation, that is, for each alternative i, $\sum_n y_{in}/N$, where y_{in} is 1 if alternative i is selected for observation n, 0 otherwise, and N is the total number of observations. We observe a great similarity in the observed proportions, except for alternatives corresponding to

Figure 15: A representative frame from the video sequences used for data collection

Nest	# steps	% of total
acceleration	1273	2.68%
constant speed	45869	96.61%
deceleration	339	0.71%
central	20950	44.12%
not central	26531	55.88%

Table 7: Number of chosen steps in each nest for Dutch data

accelerations and decelerations. This suggests that a simple model, with only alternative specific constants, may actually perform well on this data set. We show below that it is not the case.

Dataset	**extremeleft**	**left**	**front**	**right**	**extremeright**
Japanese	0.11%	3.95%	91.38%	4.39%	0.17%
Dutch	0.06%	4.40%	91.35%	4.15%	0.04%

Table 8: Comparison between Japanese and Dutch data sets for the observations proportions in the direction's cones.

We apply our model with the parameters described in Table 3 on the Dutch data set, using the Biosim package. For each observation n, we obtain a probability distribution $P_n(i)$ over the choice set.

Figure 17 represents the histogram of the probabilities $P_n(i_n^*)$ of the chosen alternatives as predicted by the model, as well as the hazard value 1/33 (where 33 is the number of alternatives) illustrating the prediction of a purely random model with equal probabilities. Again, we consider observations below this threshold as outliers. We observe that there are 2.48% of them. This is good news, as it is actually less than for the data set used for parameters estimation. The shape of the curve, as well as the low number of outliers are signs of a good performance of the model. When we compare it with the predictions obtained with the constant-only model (Figure 18), the superior forecasting potential of our model appears clearly.

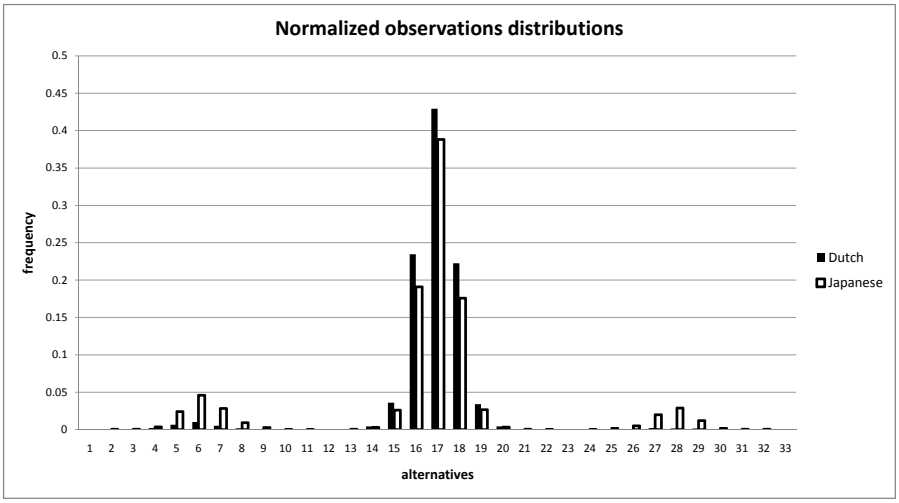

Figure 16: Comparison between the Japanese and dutch normalized observations distributions along the alternatives.

The significant superiority of our model over the constant-only model is also illustrated by comparing the proportion of outliers (2.48% vs. 10.31%) or the loglikelihood (-51647.38 vs. -77269.28, as detailed in Table 14).

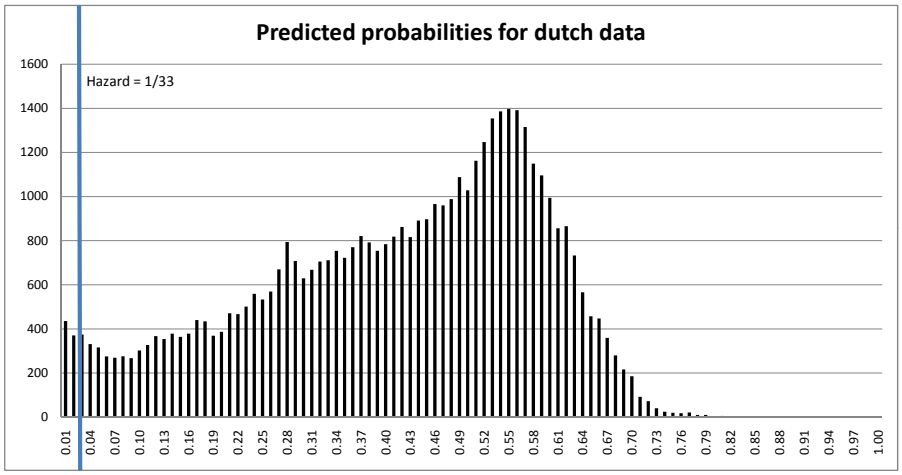

Figure 17: Prediction with the proposed model

We now compare the predictions performed by our model with the actual observations. The top part of Figure 19 reports the predicted probabilities obtained by sample enumeration, that is, for each i, $\sum_n P_n(i)$, and the bottom part the observed shares, that is $\sum_n y_{in}$. The predictions are very satisfactory, except maybe for the decelerations (alternatives 22 to 33) and accelerations (alternatives 1 to 11).

We also perform the comparison at a more aggregate level, for groups of cells. Tables 9 and 10 show a good overall performance of the model. Clearly, the `extreme left` and `extreme right` groups contain too few observations to reach any conclusion. The only bias seems to consist in a systematic over-prediction of accelerations and decelerations.

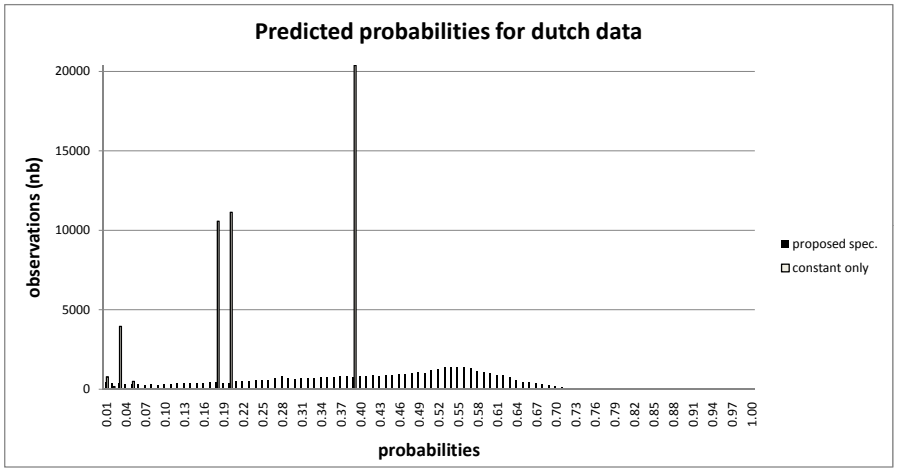

Figure 18: Prediction with the constant-only and the proposed model

Cone	Γ	M_Γ	R_Γ	$(M_\Gamma - R_\Gamma)/R_\Gamma$
Front	$5-7, 16-18, 27-29$	43619.98	43374	0.0057
Left	$3, 4, 14, 15, 25, 26$	1968.79	2089	-0.0575
Right	$8, 9, 19, 20, 30, 31$	1764.39	1972	-0.1053
Extreme left	$1, 2, 12, 13, 23, 24$	45.86	27	0.6985
Extreme right	$10, 11, 21, 22, 32, 33$	81.97	19	3.3144

Table 9: Predicted (M_Γ) and observed (R_Γ) shares for alternatives grouped by directions with the Dutch data set.

Area	Γ	M_Γ	R_Γ	$(M_\Gamma - R_\Gamma)/R_\Gamma$
acceleration	$1-11$	3892.35	1273	2.0576
constant speed	$12-22$	40733.53	45869	-0.112
deceleration	$23-33$	2855.12	339	7.4222

Table 10: Predicted (M_Γ) and observed (R_Γ) shares for alternatives grouped by speed regime with the Dutch data set.

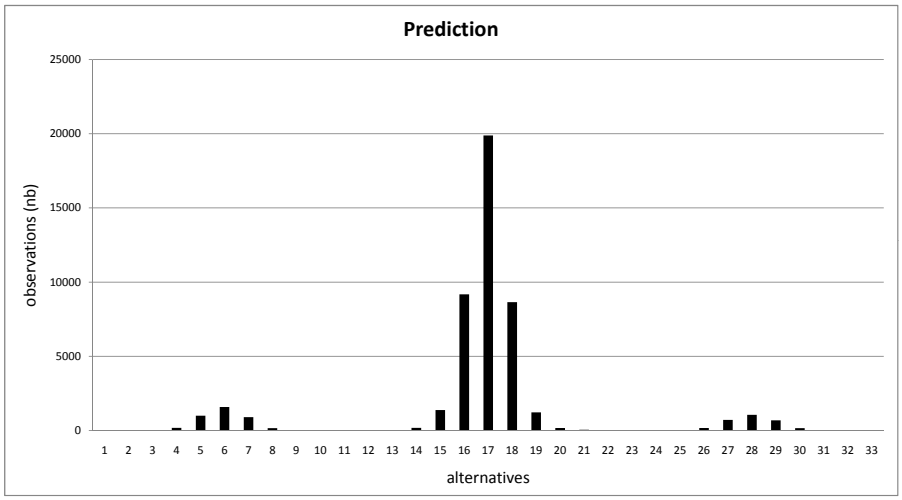

(a) Predicted

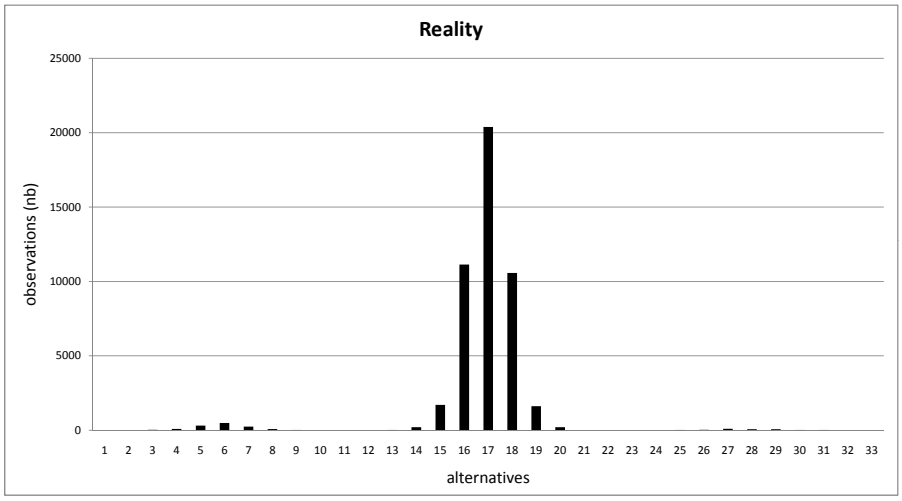

(b) Observed

Figure 19: Choice histogram predicted by the model against the revealed choices in the Dutch data set

This is consistent with the above-described analysis. The Dutch data set was collected in controlled experimental conditions, which may have introduced a bias in pedestrian behavior, depending on the exact instructions they have received. This assumption is supported by the quasi absence of decelerations in the data set, and by the different shapes of the speed distributions (see Figure 20). While the Japanese curve appears to be Gaussian, the Dutch curves contain some non-Gaussian features which are likely to be a result of the experimental nature of the data. In particular, the support is much narrower, with few high speeds. Note that, in the Japanese case, some pedestrians are running when the traffic light becomes red and the cars start moving.

Data Set	Mean speed [m/s]
Dutch (experimental)	1.297
Japanese (real)	1.341

Table 11: Average pedestrian speed in the data sets

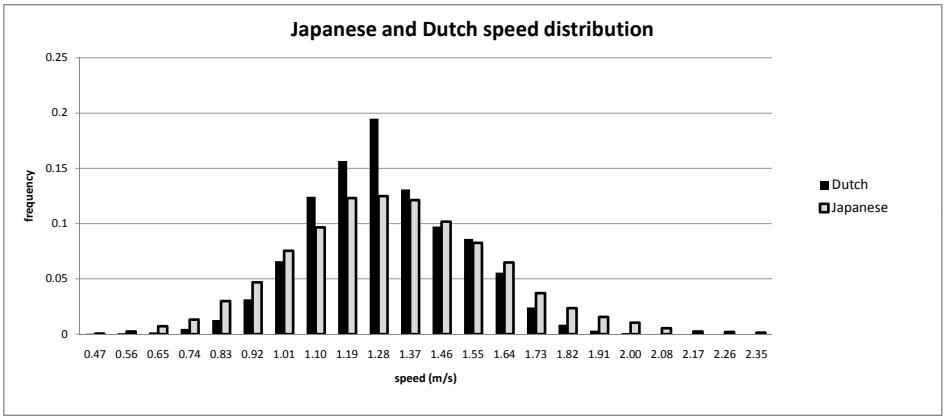

Figure 20: Distribution of speed in the two data sets

We report now the same aggregate prediction obtained with the constant-only model in Tables 12 and 13. The good performance of this simple model at the aggregate level emphasizes the need for the disaggregate validation performed above. Indeed, this apparently good performance of the model is due to the coincidental similarity of proportions of chosen alternatives in the two data sets (see Table 8). The detailed analysis presented in Figure 18 clearly rejects the simple model, while the aggregate analysis does not.

For the sake of completeness, a constant-only model has been calibrated on the Dutch data set, in the same way than for the Japanese. Our model estimated on the Japanese data is better than the constant-only model estimated on the Dutch data, when applied on the Dutch data set, both for log-likelihood (-51647.38 against -71847.69) and prediction (2.48 %, percentage of outliers against 4.33%). We have summarized the various loglikelihood values in Table 14, where each column corresponds to a model, and each row to a data set.

In summary, we observe that our model applied on the estimation data (Japanese) have few outliers compared to the constant-only model, and reproduces well the ob-

Cone	Γ	M_Γ	R_Γ	$(M_\Gamma - R_\Gamma)/R_\Gamma$
Front	$5-7, 16-18, 27-29$	43386.42	43374	0.0003
Left	$3, 4, 14, 15, 25, 26$	1877.47	2089	-0.1013
Right	$8, 9, 19, 20, 30, 31$	2082.10	1972	0.0558
Extreme left	$1, 2, 12, 13, 23, 24$	51.16	27	0.8947
Extreme right	$10, 11, 21, 22, 32, 33$	81.85	19	3.308

Table 12: Predicted (M_Γ) using the constant-only model and observed (R_Γ) shares for alternatives grouped by directions with the Dutch data set.

Area	Γ	M_Γ	R_Γ	$(M_\Gamma - R_\Gamma)/R_\Gamma$
acceleration	$1-11$	5448.24	1273	3.2798
constant speed	$12-22$	38700.42	45869	-0.1563
deceleration	$23-33$	3330.34	339	8.824

Table 13: Predicted (M_Γ) using the constant-only model and observed (R_Γ) shares for alternatives grouped by speed regime with the Dutch data set.

served choices. A forecasting cross-validation based on 80% of the sample ilustrate the good robustness of the specification. When the model is applied on the validation data (Dutch), we observe few outliers and an excellent probability histogram. Also, it reproduces very well the observed choices, in terms of directions and constant speed. We emphasize that this disaggregate analysis was necessary, as the aggregate comparison does not reject the constant-only model.

7 Conclusions

In this paper we propose a discrete choice model for pedestrian walking behavior. The short range walking behavior of individuals is modeled, identifying two main patterns: constrained and unconstrained. The constraints are generated by the interactions with other individuals. We describe interactions in terms of a leader-follower and a collision avoidance models. These models capture self-organizing effects which are characteristic of crowd behavior, such as lane formation. Inspiration for the mathematical form of these patterns is taken from driver behaviors in transportation science, and ideas such as the car following model and lane changing models have been reviewed and re-adapted to the more complex pedestrian case. The difficulties to collect pedestrian data as well as the limited information conveyed by pure dynamic data sets limit the possibilities in

Data set	Our model	Constant-only model based on Japanese data	Constant-only model based on Dutch data
Japanese	-13997.27	-17972.03	—
Dutch	-51647.38	-77269.28	-71847.69

Table 14: Loglikelihood of each model applied on the two data sets

the model specification step. Important individual effects cannot be captured without the support of socio-economic characteristics. Recent development of pedestrian laboratories, where the set up of controlled experimental conditions is possible, represents an important step in this direction. We use experimental data in a two step validation procedure. First, the model is validated on the same data set used for estimation in order to check for possible specification errors. Second, the model is run on a new data set collected at Delft University under controlled experimental conditions. The proposed validation procedure underline a good stability of the model and a good forecasting performance. Few observations are badly predicted, mostly concentrated at the extreme of the choice set. The estimated coefficients are significant and their sign is consistent with our behavioral assumptions. Differently from other previous models, we can quantify the influence of the relative kinematic characteristics of leaders and colliders on the decision maker behavior. Moreover, such quantitative analysis has been performed using real world pedestrian data.

Future developments will focus in analyzing more and improving the acceleration and deceleration patterns. In particular, we plan to investigate the use of an adaptive resolution of the choice set, as well as incorporating in the model some physical and socio-economic characteristics of the pedestrians.

Acknowledgments

We are very grateful to Kardi Teknomo and Dietmar Bauer (Arsenal Research) and Serge Hoogendoorn and Winnie Daamen (TU Delft), who provided us with the data sets. We also would like to thank Sabina Schneider, who performed the analysis for a previous version of this paper.

References

Abbe, E., Bierlaire, M. and Toledo, T. (2007). Normalization and correlation of cross-nested logit models, *Transportation Research Part B: Methodological* 41(7): 795–808.

Ahmed, K. I. (1999). *Modeling drivers' acceleration and lane changing behaviors.*, PhD thesis, Massachusetts Institute of Technology, Cambridge, MA.

Antonini, G. (2005). *A discrete choice modeling framework for pedestrian walking behavior with application to human tracking in video sequences*, PhD thesis, Ecole Polytechnique Fédérale de Lausanne. 3382.

Antonini, G. and Bierlaire, M. (2007). A discrete choice framework for acceleration and direction change behaviors in walking pedestrians, *in* N. Waldau, P. Gattermann, H. Knoflacher and M. Schreckenberg (eds), *Pedestrian and Evacuation Dynamics 2005*, Springer, pp. 145–156. ISBN:978-3-540-47062-5.

Antonini, G., Bierlaire, M. and Weber, M. (2006). Discrete choice models of pedestrian walking behavior, *Transportation Research Part B: Methodological* **40**(8): 667–687.

Antonini, G., Venegas, S., Bierlaire, M. and Thiran, J.-P. (2006). Behavioral priors for detection and tracking of pedestrians in video sequences, *International Journal of Computer Vision* **69**(2): 159–180.

Antonini, G., Venegas, S., Thiran, J.-P. and Bierlaire, M. (2004). A discrete choice pedestrian behavior model for pedestrian detection in visual tracking systems, *Proceedings of the Advanced Concepts for Intelligent Vision Systems*, Brussels, Belgium.

Bauer, D. (2007). Private communication.

Bierlaire, M. (2003). BIOGEME: a free package for the estimation of discrete choice models, *Proceedings of the 3rd Swiss Transportation Research Conference*, Ascona, Switzerland. www.strc.ch.

Bierlaire, M. (2006). A theoretical analysis of the cross-nested logit model, *Annals of Operations Research* **144**(1): 287–300.

Bierlaire, M., Antonini, G. and Weber, M. (2003). Behavioral dynamics for pedestrians, *in* K. Axhausen (ed.), *Moving through nets: the physical and social dimensions of travel*, Elsevier, pp. 1–18.

Blue, V. J. and Adler, J. L. (2001). Cellular automata microsimulation for modeling bi-directional pedestrian walkways, *Transportation Research Part B* **35**(3): 293–312.

Borgers, A. and Timmermans, H. (1986). A model of pedestrian route choice and demand for retail facilities within inner-city shopping areas, *Geographical analysis* **18**(2): 115–128.

Brady, A. T. and Walker, M. B. (1978). Interpersonal distance as a function of situationally induced anxiety, *British Journal of Social and Clinical Psychology* **17**: 127–133.

Daamen, W. (2004). *Modelling Passenger Flows in Public Transport Facilities*, PhD thesis, Delft University of Technology, The Netherlands.

Daamen, W. and Hoogendoorn, S. P. (2003). Experimental research of pedestrian walking behavior, *Transportation Research Record* **1828**: 20–30.

Dellaert, B. G., Arentze, T. A., Bierlaire, M., Borgers, A. W. and Timmermans, H. J. (1998). Investigating consumers' tendency to combine multiple shopping purposes and destinations, *Journal of Marketing Research* **35**(2): 177–188.

Dosey, M. A. and Meisels, M. (1969). Personal space and self-protection, *Journal of Personality and Social Psychology* **11**(2): 93–97.

Hartnett, J. J., Bailey, K. G. and Hartley, C. S. (1974). Body height, position, and sex as determinants of personal space, *Journal of Psychology* **87**: 129–136.

Helbing, D., Farkas, I., Molnar, P. and Vicsek, T. (2002). Simulation of pedestrian crowds in normal and evacuation simulations, *in* M. Schreckenberg and S. Sharma (eds), *Pedestrian and Evacuation Dynamics*, Springer, pp. 21–58.

Helbing, D. and Molnar, P. (1995). Social force model for pedestrian dynamics, *Physical review E* **51**(5): 4282–4286.

Herman, R. and Rothery, R. W. (1965). Car following and steady-state flow, *Proceedings on 2nd international symposium on the theory of traffic flow*, pp. 1–11.

Hoogendoorn, S., Bovy, P. and W.Daamen (2002). Microscopic pedestrian wayfinding and dynamics modelling, *in* M. Schreckenberg and S. Sharma (eds), *Pedestrian and Evacuation Dynamics*, Springer, pp. 123–155.

Horowitz, J. J., Duff, D. F. and Stratton, L. O. (1964). Body buffer zone: Exploration of personal space, *Archives of General Psychiatry* **11**(6): 651–656.

Lee, G. (1966). A generalization of linear car following theory, *Operations Research* **14**: 595–606.

McFadden, D. (1978). Modelling the choice of residential location, *in* A. Karlquist *et al.* (ed.), *Spatial interaction theory and residential location*, North-Holland, Amsterdam, pp. 75–96.

Newell, G. (1961). Nonlinear effects in the dynamics of car following, *Operations Research* **9**: 209–229.

Penn, A. and Turner, A. (2002). Space syntax based agent simulation, *in* M. Schreckenberg and S. Sharma (eds), *Pedestrian and Evacuation Dynamics*, Springer, pp. 99–114.

Phillips, J. R. (1979). An exploration of perception of body boundary, personal space, and body size in elderly persons, *Perceptual and Motor Skills* **48**: 299–308.

Sanders, J. L. (1976). Relationship of personal space to body image boundary definiteness, *Journal of Research in Personality* **10**: 478–481.

Schadschneider, A. (2002). Cellular automaton approach to pedestrian dynamics — Theory, *in* M. Schreckenberg and S. Sharma (eds), *Pedestrian and Evacuation Dynamics*, Springer, pp. 75–86.

Shapiro, R. (1978). Direct linear transformation method for three-dimensional cinematography, *Res. Quart.* **49**: 197–205.

Sommer, R. (1969). *Personal Space: The behavioral bases of design*, Prentice Hall, Englewood Cliffs, NJ.

Teknomo, K. (2002). *Microscopic Pedestrian Flow Characteristics: Development of an Image Processing Data Collection and Simulation Model*, PhD thesis, Tohoku University, Japan, Sendai.

Teknomo, K., Takeyama, Y. and Inamura, H. (2000). Review on microscopic pedestrian simulation model, *Proceedings Japan Society of Civil Engineering Conference*, Morioka, Japan.

Toledo, T. (2003). *Integrated Driving Behavior Modeling.*, PhD thesis, Massachusetts Institute of Technology, Cambridge, MA.

Toledo, T., Koutsopoulos, H. N. and Ben-Akiva, M. (2003). Modeling integrated lane-changing behavior, *Transportation Research Record* **1857**: 30–38.

Turner, A. (2001). Angular analysis, *In Proceedings 3rd International Symposium on Space Syntax*, pp. 30.1–30.11.

Venegas, S., Antonini, G., Thiran, J.-P. and Bierlaire, M. (2005). Automatic pedestrian tracking using discrete choice models and image correlation techniques, *in* B. S. and B. H. (eds), *Machine Learning for Multimodal Interaction*, Vol. 3361 of *Lecture Notes in Computer Science*, Springer, pp. 341 – 348. ISBN:978-3540245094.

Webb, J. D. and Weber, M. J. (2003). Influence of sensor abilities on the interpersonal distance of the elderly, *Environment and behavior* **35**(5): 695–711.

Wen, C.-H. and Koppelman, F. S. (2001). The generalized nested logit model, *Transportation Research Part B* **35**(7): 627–641.

Whynes, D., Reedand, G. and Newbold, P. (1996). General practitioners' choice of referral destination: A probit analysis, *Managerial and Decision Economics* **17**(6): 587.